Journal Pre-proof

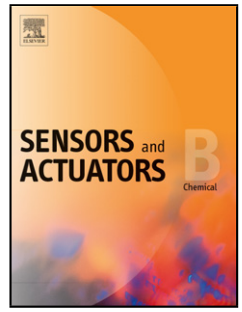

Towards a MOF e-Nose: A SURMOF Sensor Array for Detection and Discrimination of Plant Oil Scents and Their Mixtures

Salih Okur, Zejun Zhang, Mohammed Sarheed, Peter Nick, Uli Lemmer, Lars Heinke

PII: S0925-4005(19)31701-0

DOI: https://doi.org/10.1016/j.snb.2019.127502

Reference: SNB 127502

To appear in: *Sensors and Actuators: B. Chemical*

Received Date: 22 August 2019

Revised Date: 28 November 2019

Accepted Date: 29 November 2019

Please cite this article as: Okur S, Zhang Z, Sarheed M, Nick P, Lemmer U, Heinke L, Towards a MOF e-Nose: A SURMOF Sensor Array for Detection and Discrimination of Plant Oil Scents and Their Mixtures, *Sensors and Actuators: B. Chemical* (2019), doi: https://doi.org/10.1016/j.snb.2019.127502

Towards a MOF e-Nose: A SURMOF Sensor Array for Detection and Discrimination of Plant Oil Scents and Their Mixtures

Salih Okur,[a,*] Zejun Zhang,[b] Mohammed Sarheed,[c] Peter Nick,[c] Uli Lemmer[a,d] and Lars Heinke [b,*]

[a] *Karlsruhe Institute of Technology (KIT), Light Technology Institute, Engesserstraße 13, 76131, Karlsruhe, Germany*

[b] *Karlsruhe Institute of Technology (KIT), Institute of Functional Interfaces (IFG), Hermann-von-Helmholtz-Platz 1, 76344 Eggenstein-Leopoldshafen, Germany*

[c] *Karlsruhe Institute of Technology (KIT), Institute of Botanic, Molecular Cell Biology, Kaiserstr. 2, 76133, Karlsruhe, Germany*

[d] *Karlsruhe Institute of Technology (KIT), Institute of Microstructure Technology (IMT), Hermann-von-Helmholtz-Platz 1, 76344 Eggenstein-Leopoldshafen, Germany*

Corresponding Author

* Salih Okur: salih.okur@kit.edu, Lars Heinke: lars.heinke@kit.edu

Graphical abstract

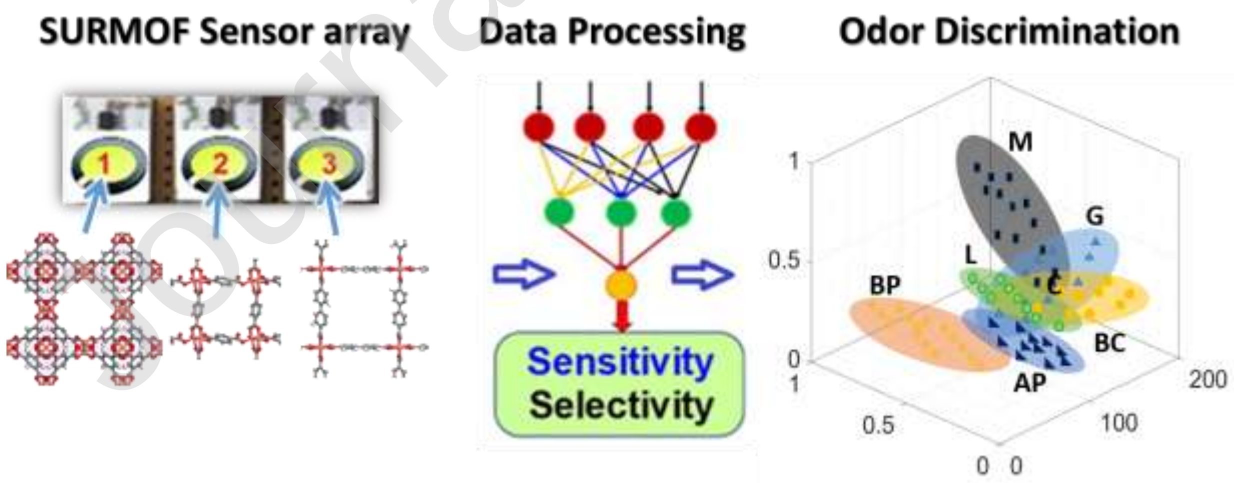

Table of content figure

Highlights:

- A QCM array comprising 3 SURMOF structures is capable of discriminating 6 plant oil scents and their binary mixtures with more than 99% prediction success at low concentration down to 1ppm.
- Simple and inexpensive setup of SURMOF-coated QCM sensors provides a high sensitivity for detecting different plant oil odors and their mixtures.

Abstract

For the sensing, detection and discrimination of odors, well-defined active layers with large specific surface areas are required. We present an array of 3 quartz crystal microbalance (QCM) sensors coated with different thin films of crystalline, highly-porous surface-mounted metal-organic frameworks (SURMOFs). The sensor array is tested for the detection and discrimination of 6 different volatile plant oil (VPO) odors as well as of their mixtures with concentrations ranging from 1 mg/L to 40 mg/L. By data analysis with machine learning algorithms, an accuracy for the classification and prediction of the different odors of 99.7% was reached. Our results show, QCM sensors coated with SURMOF films can clearly discriminate the plant oil scents and their mixtures with very high success rate at low concentrations, indicating the way towards a MOF electronic nose, MOF e-nose.

KEYWORDS. sensor array, electronic nose, metal-organic frameworks, SURMOFs, quartz crystal microbalance.

1. Introduction

The performance of sensors, in particular their sensitivity and their ability to distinguish different molecules, fundamentally depends on the active sensing material, which ideally is porous with a well-defined, large active sensing surface area.[1-3] Metal-organic frameworks (MOFs),[4, 5] a new class of nanoporous crystalline hybrid materials, seem ideally suited for improving and extending the sensor performance.[6-9] MOFs possess numerous unique properties, like a large specific surface area, a high porosity and a crystalline structure with well-defined pore space. In addition, the MOF structure can be designed and tuned by appropriate choice of components. In this way, MOF materials with very high sensitivity to various gases[10, 11] and vapors[12, 13] as well as to various compounds in solution[14, 15] were synthesized. So far, in most publications, sensors with a MOF film of a single structure has been used which typically can barely differentiate between several different molecules. Arrays of MOF films, first with two[16] later with three[15, 17] different MOF structures were used for detecting and distinguishing various pure single component gases, vapors and liquids. Mixtures of gases or odors have not yet been sensed with MOF sensor arrays.

In an “electronic noses”, e-nose,[18] gases detected by a sensor array are discriminated using machine learning techniques. The data analysis is usually based on machine learning algorithms, typically using Principal Component Analysis (PCA)[19, 20], Linear Discriminant Analysis (LDA)[21, 22] and k-Nearest Neighbor (k-NN)[23].

A challenging but relevant application for electronic noses is the detection of plant essential oils[24]. These volatile compounds are secreted by plants to modulate their interaction with other organisms. As signal molecules, they unfold their bioactivity at low concentrations (reviewed in refs. [25, 26]). Because of this functional context, these valuable plant products are relevant for use as spices and scents, but also for medicinal and agricultural purposes.[27] The composition of essential oils can vary considerably between different plant species, and even within one species, so-called chemotypes can be found. This variety of compound mixtures, along with their potent bioactivity, meaning that relevant concentrations are usually low, represents special challenges to the analytical detection of these compounds.

In the present article, we present a sensor array based on quartz crystal microbalance (QCM) sensors coated with different thin films of surface-mounted MOFs (SURMOFs).[28, 29] The sensor array consists of 3 different sensors with different response to the targeted odor molecules (α–pinene, β–pinene, linalool, menthone, β-citronellol and geraniol) as well as their binary 50% mixtures. By supervised machine-learning (classification learning) algorithms, the sensor array can clearly discriminate the different odors at different concentrations. Thus, our experimental setup presents a working e-nose for the detection and discrimination of the 6 targeted odor molecules and their mixtures. In addition, the setup is small, fitting in a cylindrical chamber with 6 cm radius and 13 cm height, see SI, and inexpensive, i.e. all components were purchased for less than 1000 € in total.

2. Methods

The MOF thin films of HKUST-1, Cu(BDC) and Cu(BPDC) structure are prepared in a layer-by-layer fashion, following previously optimized synthesis descriptions.[28] The samples were prepared by alternatively exposing the substrate to the metal node and to the linker solutions, using a spray method.[30, 31] The HKUST-1[31, 32] MOF thin film was prepared from ethanolic 1 mM copper acetate and ethanolic 0.2 mM trimesic acid (BTC) solutions; Cu(BDC)[33] from ethanolic 1 mM copper acetate and ethanolic 0.2 mM terephthalic acid (BDC) solutions and Cu(BPDC)[33] from ethanolic 1 mM copper acetate and ethanolic 0.2 mM biphenyl dicarboxylic acid (BPDC) solutions. Prior to SURMOF synthesis, the QCM substrates were functionalized by UV-ozone treatment for 30 min. All samples were prepared in 30 synthesis cycles. The crystallinity of the MOF samples with the targeted structure was investigated by X-ray diffraction, using a Bruker D8 Discovery with a wavelength of 0.154 nm.

The volatile plant oils (VPOs) used in the experiments were α-pinene (98% purity, Sigma-Aldrich), β–pinene (analytical standard, Roth, Karlsruhe), R-(+)-limonene (analytical standard, Sigma-Aldrich), linalool (97% purity, Sigma-Aldrich), menthone (analytical standard, Sigma-Aldrich), β-citronellol (analytical standard, Sigma-Aldrich), and geraniol (98% purity, Sigma-Aldrich). Here, α-pinene is abbreviated as AP, β-pinene as BP, β-citronellol as BC, geraniol as G, linalool as LN, limonene as LM and menthone as M.

The home-built setup of the 3-channel e-nose system as well as the gas delivery system with a micro-liter syringe pump for odors concentration control is described in the supporting information, SI1. The frequency shift of each quartz sensor with an AT-cut and a resonance frequency of 10 MHz was recorded. For the QCM data collection, 5V/16MHz ATMega32U4 microcontrollers and open source Pierce oscillator circuits designed by openQCM have been used.[34] 3 data sets were recorded per second. Temperature and humidity were measured with an Adafruit HTU21D-F sensor. The entire setup has been computer controlled with a program code written in MATLAB.

The odors were evaporated at 60°C during the injection into the test chamber with a bulb filament heater. Two valves with mass flowmeters were used to transfer the evaporated odorant gases through the test cell. A stainless steel cylindrical test cell with a volume of 0.5 L has been kept at a constant temperature of (34 ± 1)°C to prevent condensation of gas molecules on the wall of the test chamber. The different VPOs with concentrations between 1mg/L – 40mg/L (i.e., 1.0, 5.0, 10, 20, 30, 40mg/L) have been injected sequentially into the sample evaporator attached to the test cell with a computer-controlled microliter syringe (Hamilton Model 700).

For the desorption/activation process, the test chamber was purged with dry air with a flow rate of 5 L min^{-1} for 16.5 min before introducing the evaporated gas samples. In the experiments, each cycle of concentration measurement consists of 8.5 min for adsorption and 16.5 min for desorption, i.e. 25 min in total. The initial resonance frequency values of each sensor were determined at the beginning of the experiment as an average value of 10 measurements. The shift in the resonance frequency due to the uptake of the targeted molecules was recorded as response of each sensor during the experiments.

The change of the mass density (Δm) of the film on the surface is calculated by the Sauerbrey equation[35]:

$$\Delta m = \frac{A\sqrt{\mu\rho}}{2\,{f_0}^2} \times \Delta f$$

where f_0 denotes the resonance frequency of the fundamental mode of the QCM crystal, Δf is the frequency change, A the surface area, ρ the density of the crystal (2.684 g cm^{-3}) and μ is the shear modulus of quartz (2.947×10^{11} g cm^{-1} s^{-2}).

Standard machine learning algorithms, that are k-Nearest Neighbor (k-NN)[36, 37] but also Principal Component Analysis (PCA) and Linear Discriminant Analysis (LDA) [21, 22] algorithms written in MATLAB, have been used for classifying the sensing data. During data analysis, more than 100 data points of the maximum resonance frequency shifts are used for the classification algorithms. This makes 2638 observation points. 10 folds cross-validation was used for the classification methods with 2374 observations for training sets and 264 observations for the test sets.

3. Results and discussion

The structure of the SURMOF films are shown in Figure 2. The X-ray diffraction data of the samples verify the targeted SURMOF structures. The HKUST-1 thin film has an isotropic, 3-dimensional pore structure with pore windows of approximately 1 nm diameter.[32] The Cu(BDC) and Cu(BDPC) films are composed of 2d-MOF sheets forming 1-dimensional channels. The pore size is approximately 1 nm and 1.4 nm for Cu(BDC) and Cu(BDPC), respectively.[33]

Before investigating the sensing of mixtures, we have investigated the response of the SURMOF-coated QCM array towards the exposure to the different odor molecules of various concentrations in their pure form. The frequency shifts of the SURMOF-coated QCM sensor array versus time as responses to the 6 different plant oils with the concentration ranging between 1 mg/L – 40 mg/L are shown in Figure 3. The recorded frequency shifts of the different sensors clearly differ from each other. For example, while the maximum frequency shift for Cu(BPDC) reaches 1600 Hz for geraniol, the frequency shift of the HKUST-1- and Cu(BDC)-coated sensors are only in the order of 200 Hz, see Figure 3a. Due to the different affinity of the odor molecules to the host MOF film, the frequency shifts are substantially different for each guest molecule. The linearity of the response over the entire tested working range, that is 1 to 40 mg/L, can be seen in Figure SI9. In addition, the slopes of the frequency shift versus concentration (table 1), which is related to the sensitivity of the sensor to the VPOs, significantly differ. The highest sensitivity has been obtained for Cu(BPDC) to geraniol. The lowest sensitivity was obtained from HKUST-1 to α-pinene. We assume that the different sensitivities result from the different strengths of the attractive adsorption sites, which are close to the metal nodes (based on polar interactions) and close the phenyl rings of the linker (based on π interactions). It should be noted that even for the smallest tested concentration, 1 mg/L, all sensors show a clear response.

The repeatability of the sensor setup is investigated by repeating the same experiment 4 times, see table SI3. The standard deviations between the responses of the different experiments is in the range of 0.1 to 0.2 Hz, which is significantly smaller than the signal of the odors. Thus, it demonstrates the reproducibility and high signal-to-noise ratio. Repeating the experiments after many months, table SI4, shows only minor deviations from the initial results, demonstrating the stability of the sensor setup.

Table 1: The slops of the linear fits to the frequency shifts versus concentrations between 1mg/L and 40 mg/L, see Figure SI9.

VPO	**Cu(BDC)** [Hz / (mg L^{-1})]	**Cu(BPDC)** [Hz / (mg L^{-1})]	**HKUST-1** [Hz / (mg L^{-1})]
Geraniol	-9.3	-39.7	-3.7
β-Citronellol	-4.9	-23.7	-3.8
α-Pinene	-0.6	-3.9	-1.2
β-Pinene	-0.83	-5.8	-1.6
Linalool	-0.4	-5.0	-0.9
Menthone	-1.2	-6.1	-0.6

A 3D-plot of the frequency shifts as response to the odors is shown in Figure 4a. Different odor molecules can be clearly distinguished, with only a minute interference between the data points. The sensor responses to the geraniol and β-citronellol are relatively high compared to the other odor molecules, indicating their high affinity towards the MOF structures.

Figure 4b shows a radar plot of the sensor performance for the pure odors of 1 mg/L concentration. In general, the response of Cu(BPDC) is higher than both Cu(BDC) and HKUST-1, where Cu(BDC) shows often the smallest response.

For classifying the sensor data, a machine learning algorithm was used. With the k-nearest neighbor (k-NN) classification approach, the number of nearest neighbors, type of distance metrics and weighting function are crucial parameters. In this work, the number of nearest neighbors was chosen as k=10 and a pairwise Euclidean distance metrics with the squared inverse weighting function (weight is 1/distance^2) was used. A detailed comparison with other weight functions such as cosine or cubic as well as with other algorithms is given in in the supporting information, SI2 and table SI1.

Figure 5 shows the weighted k-NN analysis results for the 6 different pure VPOs at 1 mg/L. The VPOs can be clearly distinguished from each other and they can be grouped. Based on this analysis, Figure 6a shows the confusion matrix for the weighted k-NN of pure VPOs with 6 classes. The 6 different pure VPOs were classified with almost 100% accuracy with 9116 observations (with 8205 training sets and 911 test sets, see SI). This means there is essentially no interference between the sensor responses of the different VPOs and the sensor array shows no crosstalk.

For testing the sensor setup and the analysis algorithm, a new set of experiments was performed where the sensors were exposed to the pure VPO without beforehand stating which VPO it is. The test data, plotted as crosses in Fig. 5, can be clearly assigned to the respective molecules. It shows that all VPOs can be undoubtedly and reproducibly distinguished.

The sensing performance towards mixtures was investigated by exposing the sensors to the 50% binary mixtures of the VPOs, see SI3. The results were analyzed in the same way as the pure-VPO-results. The confusion matrix of the VPOs and their mixtures with 17 classes at 1mg/L are shown in Fig 6b. There, 98.4% accuracy has been obtained for the mixtures with 17 classes (6 pure and 11 mixtures where all concentrations are summarized in one class) and 3131 observations (with 2818 training sets and 313 test sets, see SI6). This shows that a SURMOF-sensor array can discriminate VPOs and their mixtures down to 1mg/L sensitivity for single concentration.

The weighted k-NN analysis results for 6 different VPOs and their 50% mixtures at 6 different concentrations with 102 classes (i.e. the different concentrations of the same mixtures are in separate classes) is shown in SI7.

The comparison of the results from different analysis algorithms, LDA, PCA, k-NN and weighted k-NN for 6 different VPOs and their 50% mixtures at 6 different concentrations with 102 classes (see supporting information, SI and table SI2) shows that all algorithms deliver very precise results. The highest precision, that means the clearest discrimination between the different odors, was obtained with the weighted k-NN algorithm.

For the performance evaluation of the e-nose, the effect of the sensor numbers used for discrimination was investigated. Figure 7 shows the accuracy of the VPO detection determined by the weighted k-NN algorithm with increasing number of sensors used for discrimination for all the pure odors and their mixtures with 17 classes without concentration classification. The discrimination accuracy is 26.3% for just 1 single sensor, here Cu(BDC), 89.9% for 2 sensors (Cu(BDC) and Cu(BPDC)) and 99.7% for all 3 sensors. Similar calculations have been done with LDA and k-NN with different weight functions. Detailed accuracy calculations for all the other concentrations between 1mg/L and 40 mg/L are given in table SI2. These results are in agreement with theoretical predictions of the sensing performance of MOF arrays of different sizes for the detection of gases such as methane.[38]

4. Conclusion

An array of 3 QCM sensors coated with nanoporous thin films of metal-organic frameworks with HKUST-1, Cu(BDC) and Cu(BPDC) structures has been used to discriminate 6 different volatile plant oils, α-pinene, β-pinene, linalool, menthone, β-citronellol, and geraniol, and their 50% mixtures. The concentrations range from 1mg/L to 40mg/L. The datasets obtained from each sensor were used for the prediction using k-nearest-neighbors (k-NN) techniques with an accuracy of the classification of 99.7%. The k-NN analysis results show that QCM array comprising 3 SURMOF structures is capable of discriminating plant oil scents and their binary mixtures with practically perfect success rates.

The study shows that the simple and inexpensive setup of SURMOF-coated QCM sensors provides a sufficient sensitivity for detecting different plant oil odors and their mixtures. Combined with the appropriate analysis algorithms, it allows the classification and discrimination. We foresee that increasing the number of sensors and using more specialized MOF thin films with more specific interaction towards the targeted molecules will enable to exploit the full potential of SURMOF-coated-QCM-e-noses to discriminate various molecules, in particular hard to distinguish molecules like different isomers.

Author Contributions: All authors have given approval to the final version of the manuscript.

Declaration of interests

☒ The authors declare that they have no known competing financial interests or personal relationships that could have appeared to influence the work reported in this paper.

☐The authors declare the following financial interests/personal relationships which may be considered as potential competing interests:

5. Funding sources

This work is financially supported by the Alexander von Humboldt Foundation, the German Research Foundation (HE-7036/5) and the Chinese Science Council.

Acknowledgment

The authors, in particular S.O., gratefully thank the Alexander von Humboldt Foundation.

Supporting Information:

Setup description, details of machine learning algorithms, QCM data and analysis.

References

[1] D. James, S.M. Scott, Z. Ali, W.T. O'Hare, Chemical sensors for electronic nose systems, Microchim. Acta, 149 (2005) 1-17.
[2] E.A. Baldwin, J. Bai, A. Plotto, S. Dea, Electronic Noses and Tongues: Applications for the Food and Pharmaceutical Industries, Sensors, 11 (2011) 4744-4766.
[3] G.J. Li, X.H. Zhang, S. Kawi, Relationships between sensitivity, catalytic activity, and surface areas of SnO gas sensors, Sens. Actuator B-Chem., 60 (1999) 64-70.
[4] S. Kaskel, The Chemistry of Metal-Organic Frameworks: Synthesis, Characterization, and Applications, Wiley2016.
[5] H. Furukawa, K.E. Cordova, M. O'Keeffe, O.M. Yaghi, The Chemistry and Applications of Metal-Organic Frameworks, Science, 341 (2013) 1230444.
[6] I. Stassen, N.C. Burtch, A.A. Talin, P. Falcaro, M.D. Allendorf, R. Ameloot, An updated roadmap for the integration of metal-organic frameworks with electronic devices and chemical sensors (vol 46, pg 3185, 2017), Chem. Soc. Rev., 46 (2017) 3853-3853.

[7] F.Y. Yi, D.X. Chen, M.K. Wu, L. Han, H.L. Jiang, Chemical Sensors Based on Metal-Organic Frameworks, ChemPlusChem, 81 (2016) 675-690.
[8] A. Chidambaram, K.C. Stylianou, Electronic metal-organic framework sensors, Inorganic Chemistry Frontiers, 5 (2018) 979-998.
[9] L. Heinke, M. Tu, S. Wannapaiboon, R.A. Fischer, C. Wöll, Surface-mounted metal-organic frameworks for applications in sensing and separation, Micropor. Mesopor. Mat., 216 (2015) 200-215.
[10] O. Yassine, O. Shekhah, A.H. Assen, Y. Belmabkhout, K.N. Salama, M. Eddaoudi, H2S Sensors: Fumarate-Based fcu-MOF Thin Film Grown on a Capacitive Interdigitated Electrode, Angewandte Chemie International Edition, 55 (2016) 15879-15883.
[11] S. Achmann, G. Hagen, J. Kita, I.M. Malkowsky, C. Kiener, R. Moos, Metal-Organic Frameworks for Sensing Applications in the Gas Phase, Sensors, 9 (2009) 1574-1589.
[12] A.L. Robinson, V.L. Stavila, T.R. Zeitler, M.I. White, S.M. Thornberg, J.A. Greathouse, M.D. Allendorf, Ultrasensitive Humidity Detection Using Metal-Organic Framework-Coated Microsensors, Analytical Chemistry, 84 (2012) 7043-7051.
[13] I. Ellern, A. Venkatasubramanian, J.-H. Lee, P. Hesketh, V. Stavila, A. Robinson, M. Allendorf, HKUST-1 coated piezoresistive microcantilever array for volatile organic compound sensing, Micro & Nano Letters, 8 (2013) 766-769.
[14] M. Jurcic, W.J. Peveler, C.N. Savory, D.-K. Bucar, A.J. Kenyon, D.O. Scanlon, I.P. Parkin, Sensing and Discrimination of Explosives at Variable Concentrations with a Large-Pore MOF as Part of a Luminescent Array, ACS App. Mat. Int., 11 (2019) 11618-11626.
[15] L. Qin, X. Wang, Y. Liu, H. Wei, 2D-Metal-Organic-Framework-Nanozyme Sensor Arrays for Probing Phosphates and Their Enzymatic Hydrolysis, Analytical Chemistry, 90 (2018) 9983-9989.
[16] T. Lee, Z.X. Liu, H.L. Lee, A Biomimetic Nose by Microcrystals and Oriented Films of Luminescent Porous Metal-Organic Frameworks, Crystal Growth & Design, 11 (2011) 4146-4154.
[17] M.G. Campbell, S.F. Liu, T.M. Swager, M. Dinca, Chemiresistive Sensor Arrays from Conductive 2D Metal-Organic Frameworks, J. Am. Chem. Soc., 137 (2015) 13780-13783.
[18] A. Loutfi, S. Coradeschi, G.K. Mani, P. Shankar, J.B.B. Rayappan, Electronic noses for food quality: A review, Journal of Food Engineering, 144 (2015) 103-111.
[19] A.L. Price, N.J. Patterson, R.M. Plenge, M.E. Weinblatt, N.A. Shadick, D. Reich, Principal components analysis corrects for stratification in genome-wide association studies, Nature Genetics, 38 (2006) 904-909.
[20] H. Abdi, L.J. Williams, Principal component analysis, Wiley Interdisciplinary Reviews: Computational Statistics, 2 (2010) 433-459.
[21] S.J.D. Prince, J.H. Elder, Probabilistic Linear Discriminant Analysis for Inferences About Identity, 2007 IEEE 11th International Conference on Computer Vision, 2007, pp. 1-8.
[22] P. Shaoning, S. Ozawa, N. Kasabov, Incremental linear discriminant analysis for classification of data streams, IEEE Transactions on Systems, Man, and Cybernetics, Part B (Cybernetics), 35 (2005) 905-914.
[23] E.-H. Han, G. Karypis, V. Kumar, Text Categorization Using Weight Adjusted k-Nearest Neighbor Classification, Springer Berlin Heidelberg, Berlin, Heidelberg, 2001, pp. 53-65.
[24] S. Kiani, S. Minaei, M. Ghasemi-Varnamkhasti, Application of electronic nose systems for assessing quality of medicinal and aromatic plant products: A review, Journal of Applied Research on Medicinal and Aromatic Plants, 3 (2016) 1-9.
[25] I.T. Baldwin, R. Halitschke, A. Paschold, C.C. von Dahl, C.A. Preston, Volatile Signaling in Plant-Plant Interactions: "Talking Trees" in the Genomics Era, Science, 311 (2006) 812-815.
[26] M.E. Maffei, J. Gertsch, G. Appendino, Plant volatiles: Production, function and pharmacology, Natural Product Reports, 28 (2011) 1359-1380.
[27] S. Burt, Essential oils: their antibacterial properties and potential applications in foods—a review, International Journal of Food Microbiology, 94 (2004) 223-253.
[28] O. Shekhah, H. Wang, S. Kowarik, F. Schreiber, M. Paulus, M. Tolan, C. Sternemann, F. Evers, D. Zacher, R.A. Fischer, C. Wöll, Step-by-step route for the synthesis of metal-organic frameworks, J. Am. Chem. Soc., 129 (2007) 15118-15119.

[29] L. Heinke, C. Wöll, Surface-Mounted Metal–Organic Frameworks: Crystalline and Porous Molecular Assemblies for Fundamental Insights and Advanced Applications, Adv. Mater., 31 (2019) 1806324.
[30] H.K. Arslan, O. Shekhah, J. Wohlgemuth, M. Franzreb, R.A. Fischer, C. Wöll, High-Throughput Fabrication of Uniform and Homogenous MOF Coatings, Adv. Funct. Mater., 21 (2011) 4228-4231.
[31] S. Hurrle, S. Friebe, J. Wohlgemuth, C. Wöll, J. Caro, L. Heinke, Sprayable, Large-Area Metal–Organic Framework Films and Membranes of Varying Thickness, Chem. Eur. J., 23 (2017) 2294-2298.
[32] S.S.Y. Chui, S.M.F. Lo, J.P.H. Charmant, A.G. Orpen, I.D. Williams, A chemically functionalizable nanoporous material Cu-3(TMA)(2)(H2O)(3) (n), Science, 283 (1999) 1148-1150.
[33] J.X. Liu, B. Lukose, O. Shekhah, H.K. Arslan, P. Weidler, H. Gliemann, S. Bräse, S. Grosjean, A. Godt, X.L. Feng, K. Mullen, I.B. Magdau, T. Heine, C. Wöll, A novel series of isoreticular metal organic frameworks: realizing metastable structures by liquid phase epitaxy, Scientific Reports, 2 (2012) 921.
[34] C.A. E. S. Muckley, C. B. Jacobs, T. Hianik and I. N. Ivanov, In Low-Cost Scalable Quartz Crystal Microbalance Array for Environmental Sensing, SPIE Organic Photonics+Electronics, Int. Soc. Opt. Photonics, DOI 10.1117/12.2237942(2016) 99440Y
[35] G. Sauerbrey, G. Jung, Vibrational Modes of Planoconvex Quartz Plates, Z Angew Physik, 24 (1968) 100-+.
[36] S. Guney, A. Atasoy, Multiclass classification of n-butanol concentrations with k-nearest neighbor algorithm and support vector machine in an electronic nose, Sens. Actuator B-Chem., 166 (2012) 721-725.
[37] K.T. Tang, Y.S. Lin, J.M. Shyu, A Local Weighted Nearest Neighbor Algorithm and a Weighted and Constrained Least-Squared Method for Mixed Odor Analysis by Electronic Nose Systems, Sensors, 10 (2010) 10467-10483.
[38] J.A. Gustafson, C.E. Wilmer, Computational Design of Metal Organic Framework Arrays for Gas Sensing: Influence of Array Size and Composition on Sensor Performance, J. Phys. Chem. C, 121 (2017) 6033-6038.

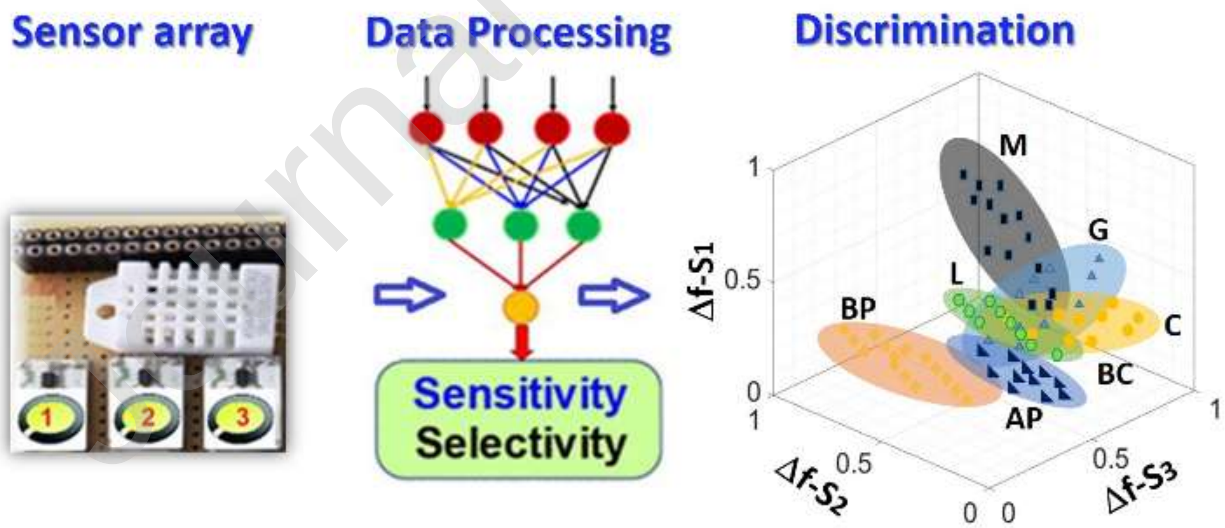

Figure 1: Scheme of the MOF e-nose. An array of QCM sensors coated with SURMOFs

is used to detect various odors. By machine-learning-data-processing, the different odor molecules as well as their mixtures can be detected and clearly distinguished.

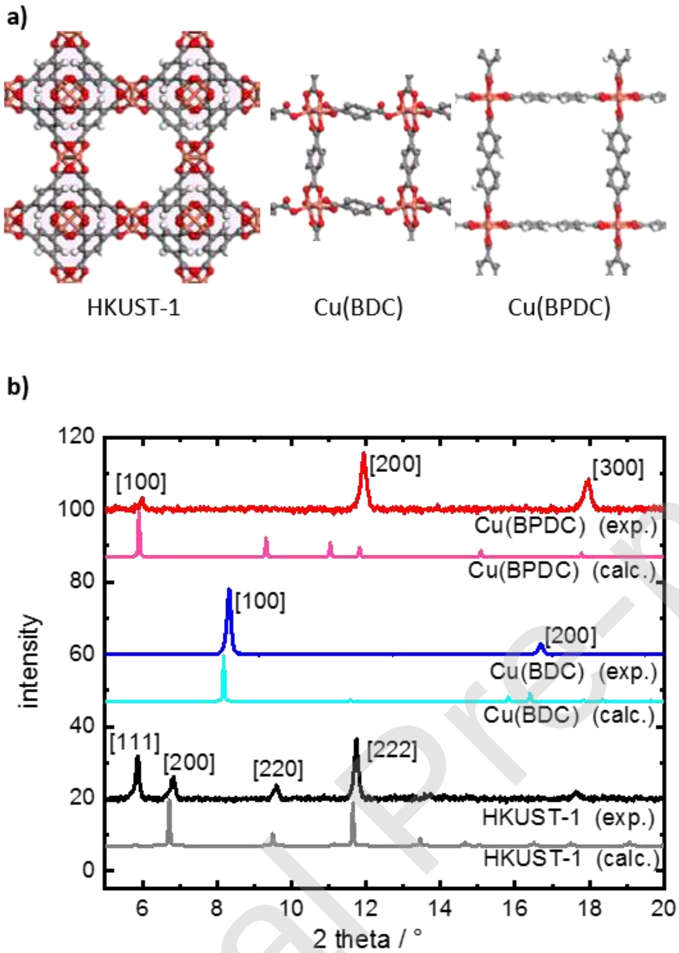

Figure 2: Sketch of the SURMOF structures (a) with the X-ray diffractograms (b). The name of the structures as well as the diffraction peaks are labelled. The calculated XRDs of the targeted structures are shown below the measured XRDs.

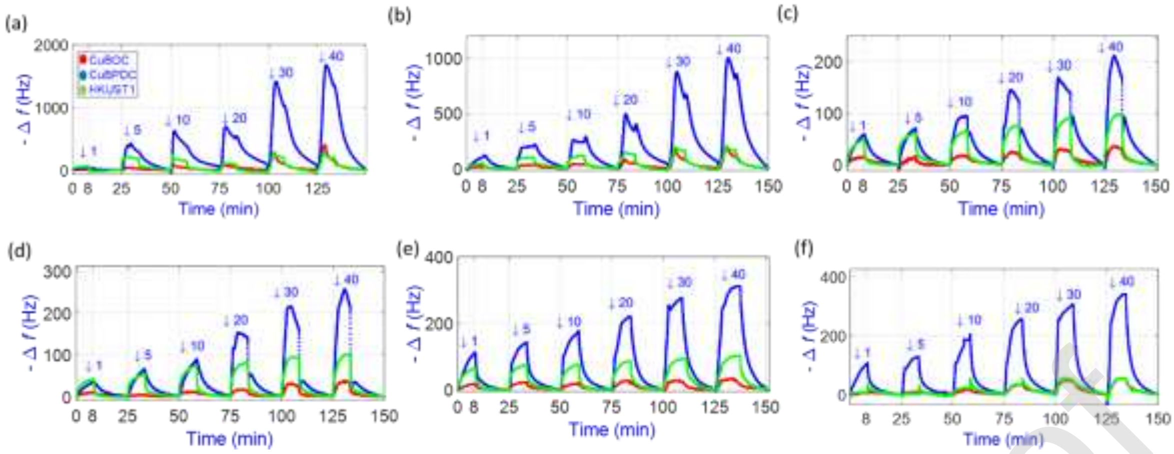

Figure 3: Frequency shifts versus time for the different SURMOF-coated QCM sensors of the e-nose as responses to the vapors of the 6 different plaint oils: geraniol (a), β-citronellol (b), α-pinene (c), β-pinene (d), linalool (e) and menthone (f) with the concentration range of 1 mg/L – 40 mg/L (see labels). The HKUST-1-coated sensor is plotted in green, Cu(BPDC) in blue and Cu(BDC) in red.

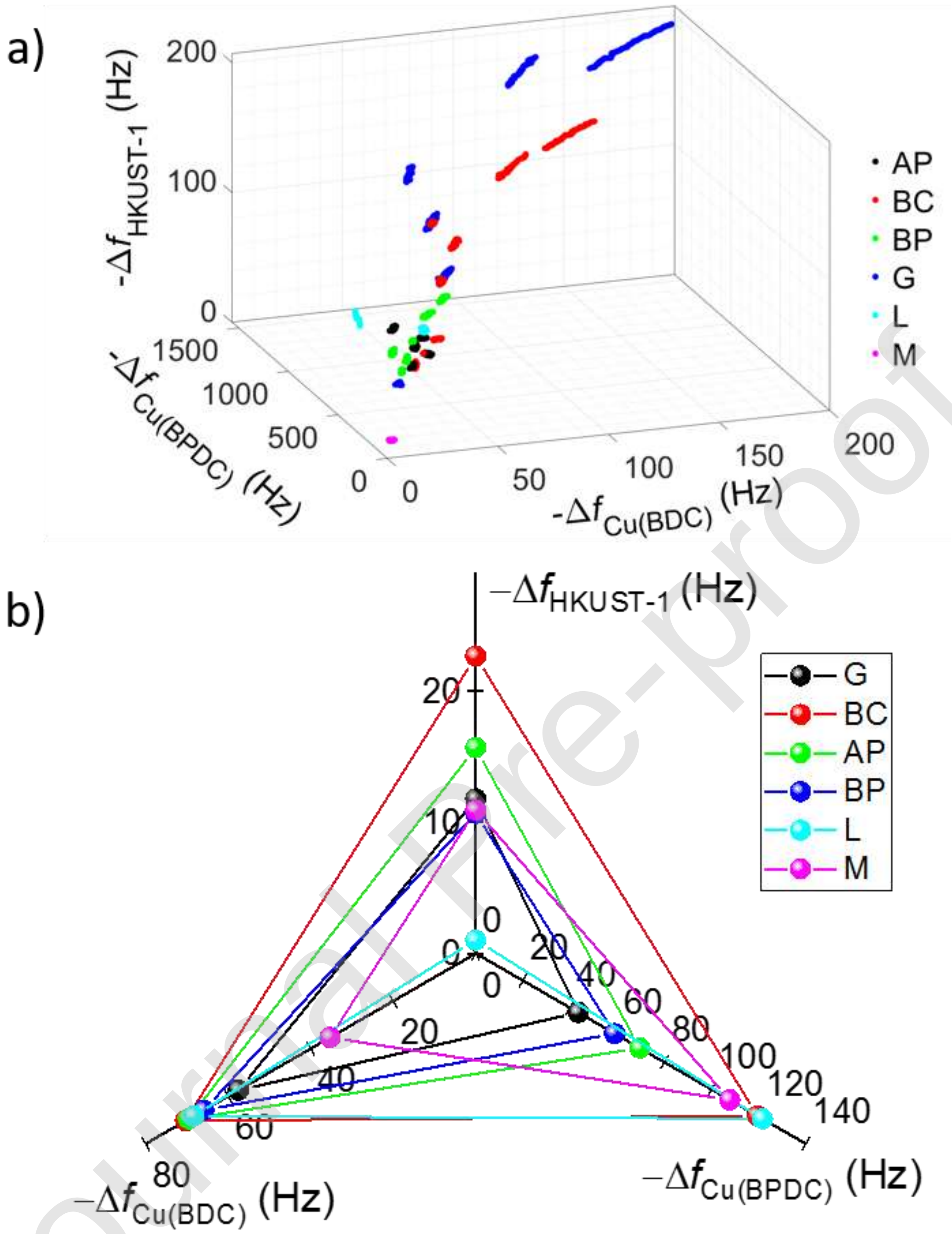

Figure 4: a) 3D plot of the QCM frequency shifts for all pure molecules at all investigated concentrations. The *x*, *y* and *z* axes are the responses from the HKUST-1, Cu(BDC) and Cu(BPDC) sensors, respectively. b) Radar plot of the frequency shifts of the HKUST-1, Cu(BDC) and Cu(BPDC) sensors for all the pure molecules at 1 mg/L concentration.

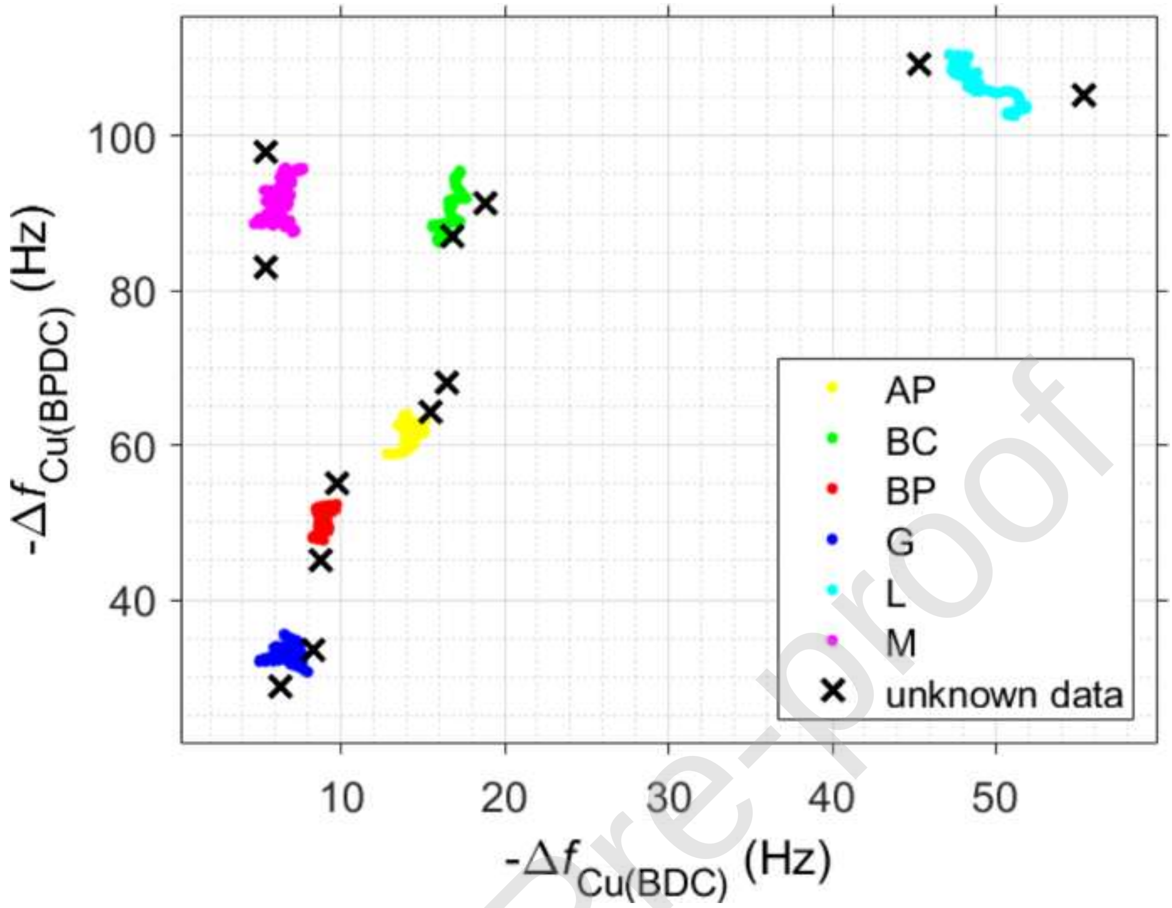

Figure 5: Discrimination and grouping of the sensor data for pure VPOs at 1 mg/L by the k-NN algorithm. The grouped 6 different VPO classes are represented with different colors, see legend. The sensing results of the "unknown" molecules are plotted as x and were correctly assigned. For sake of clarity, the results of only 2 sensors (Cu(BPDC) and Cu(BDC)) are shown.

a)

b)

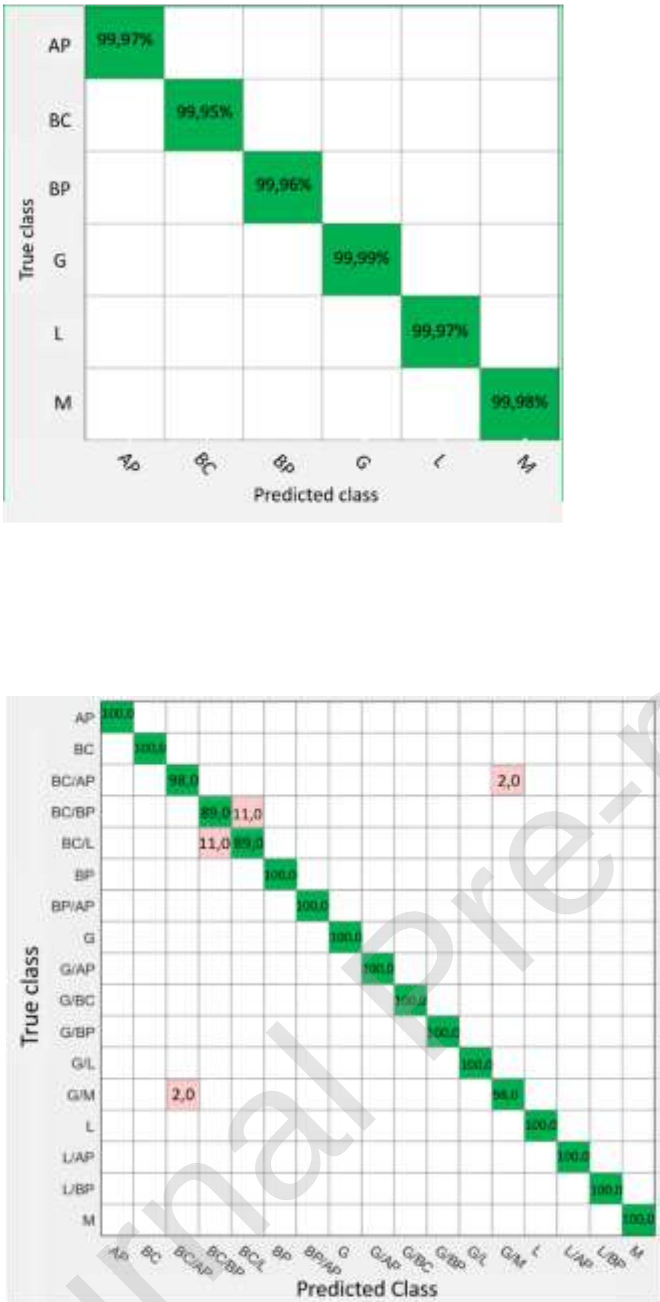

Figure 6: The confusion matrices for the weighted k-NN of pure VPOs with 6 classes (a) and of VPOs and their (50%) mixtures with 17 classes (b) at 1mg/L.

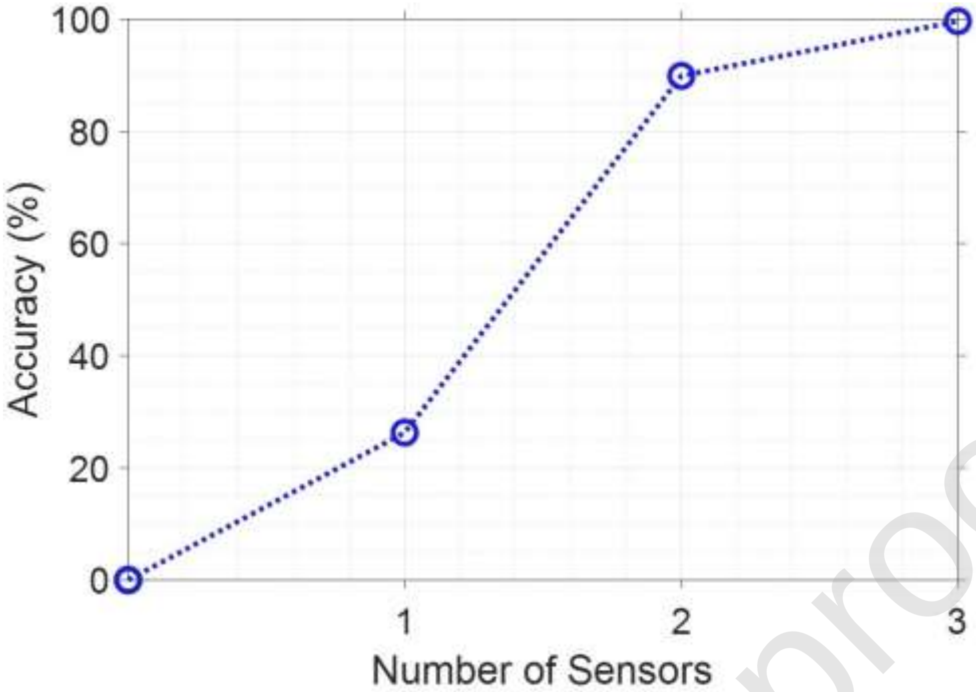

Figure 7: Accuracy of determining the correct results with the weighted k-NN algorithm for different numbers of sensors. Here, the accuracy of the discrimination for all pure VPOs and their mixtures with 17 classes (without concentration classification) is presented. 1 sensor is Cu(BDC), 2 sensors are Cu(BDC) and Cu(BPDC) as well as for all 3 sensors.